Article ID: 1003－6326(2005)04－0897－05

Electrocrystallization nucleation and growth of NiFe alloys on brass substrate①

ZHANG Zhao(张 昭)
(Department of Chemistry, Zhejiang University, Hangzhou 310027, China)

Abstract: The electrocrystalliztion nucleation and growth process of Ni-Fe alloy was studied using cyclic voltammetry and chronoamperometry. The results show that, in the case of high deposition overpotential, the nucleation/growth process of Ni-Fe binary alloy is 3-D instantaneous, and the growth rate of the previously formed nuclei increases with overpotential. However, at low overpotential, no distinguished nucleation current can be observed. Meanwhile, the discrepancy between the experimental non-dimensional variables $(I/I_m)^2$ and those calculated from the theoretical model was elucidated in the light of the molecular orbital theorem.

Key words: nickel-iron electroplating; nucleation; growth; mechanism
CLC number: O 646.6 **Document code:** A

1 INTRODUCTION

Electrodeposited Ni-Fe alloy was widely used in the area of memory devices for computers, as perpendicular magnetic recording media for rotary encoders and as stampers for disk pressing[1]. Meanwhile, due to the substitution of nickel by iron, less expensive Ni-Fe alloy with high corrosion resistance may be an alternative for widely used pure nickel coatings. So far, many attempts have been made to study the influence of technological parameters on the composition and structure of Ni-Fe alloys[1-7], investigate the electrocrystallization process[8], and model the galvanostatic pulse and pulse reverse plating of Ni-Fe alloys on a rotating disk electrode[9, 10].

Up to date, Ni-Fe alloy can be obtained by many deposition techniques. Among them, electrodeposition offers unique possibility for an exact and easy control of the deposition conditions, the chemical composition and the microstructure of the electrodeposited layer, and represents a straightforward approach for locally structuring and modifying surfaces[11]. During the whole electroplating process, the nucleation kinetics and the growth mechanism of the first metallic nuclei formed on the initial substrate are critical steps, which determine the physicochemical properties of the electrodeposited materials[12, 13]. Electrocrystallization on different substrates is commonly related to only one kind of nucleation process[14-16] and complex deposition system, consisting of two or more nucleation processes with sophisticated transitions between the different types[17].

Generally, characterization of electrocrystallization nucleation and growth process is performed by analyzing the cyclic voltammograms and the current transients obtained using chronoamperometry technique. So far, a number of different theoretical formalisms have been developed to identify the different nucleation process and different growth types[17-23].

The goal of this paper is to probe into the electrocrystallization nucleation/growth processes of Ni-Fe alloys in chloride-boric acid solution, and find the basis for further studying the electrodeposition mechanism of nanocrystallization ternary CoNiFe soft magnetic alloys.

2 EXPERIMENTAL

The experimental electrolyte was prepared with AR grade reagents and twice distilled water according to the basic compositions listed in Table 1. A conventional three-electrode system consisting of 1) cycloidal polycrystalline brass electrode with an area of 0.502 7 cm^2 exposed as working electrode(WE), 2) saturated calomel(reference) electrode(SCE) and 3) a large bright platinum foil as the counter electrode, was employed. Before measurement, the exposed surface of the WE was polished with silicon carbide papers and velvet, rinsed with the twice distilled water, washed in acetone, rinsed with the twice distilled water again and then dried in air. Cyclic voltammetry and chronoamperometry were performed with a commercial electrochemical analyzer/workstation (IM6e, Germany). The experimental temperature was

① **Foundation item:** Projects(20203015, 50499335) supported by the National Natural Science Foundation of China; Project supported by the State Key Laboratory for Corrosion and Protection, China **Received date:** 2004－12－29; **Accepted date:** 2005－05－09
Correspondence: ZHANG Zhao, PhD, Associate Professor; Tel: +86-571-87952318; E-mail: eaglezzy@zjuem.zju.edu.cn

Table 1 Basic electrolyte compositions and experimental conditions for electroplating nickel-iron alloys

Components/(g·L^{-1})							pH	Rotating speed of solution/(r·min^{-1})
$NiSO_4 \cdot 6H_2O$	$FeSO_4 \cdot 7H_2O$	H_3BO_3	NH_4Cl	Na_2SO_4	Ascorbic acid	Additive		
52.5	8.7	40	30	14	1.0	0.01	2.66	1 000

(25±1) ℃ controlled by thermostat water tank, and all potentials were referred to SCE.

3 RESULTS AND DISCUSSION

3.1 Voltammetric study

During cyclic voltammetric experiments, the sweep potential range was from open circuit potential(c.a. −0.252 V) to −1.6 V and always initiated in the negative direction. Fig. 1 shows the typical voltammogram obtained in Ni-Fe electroplating solution with a scanning rate of 10 mV/s.

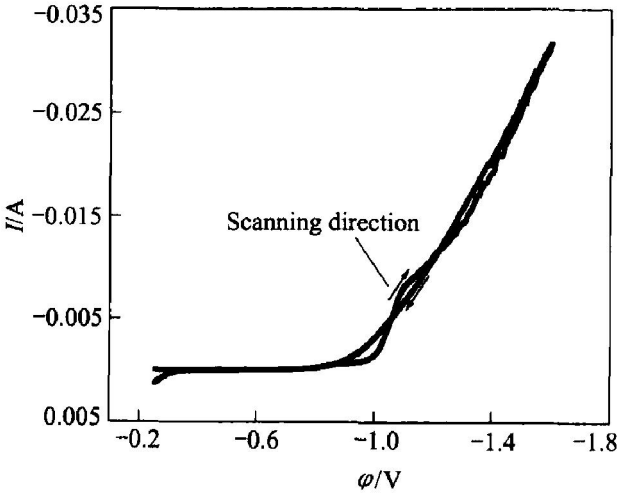

Fig. 1 Typical voltammogram for brass electrode in basic Ni-Fe binary electroplating solution

It can be seen that there exist current loops in anodic branch of voltammogram, which imply that the electrodeposition of Ni-Fe alloy follows three-dimensional (3-D) nucleation and grain growth mechanism[24, 25].

3.2 Chronoamperometric study

Fig. 2 shows the experimental current—time transient curves. It can be seen that, each of the "I—t" curves consists of an initial spike(within the first 0.02 s) due to the charging of the electrochemical double layer, a subsequently rising portion due to the nucleation process and a posterior decreasing portion due to the diffusion process. The rising section appears to reach its maximum at increasingly shorter time with more negative overpotential steps. The maximum in the current transient corresponds to the maximum surface area, i.e. the point with hemi-spherical nuclei is on the point of collision.

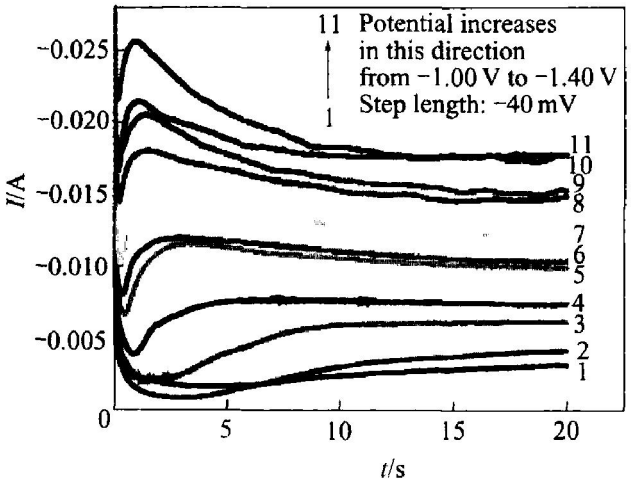

Fig. 2 Potentiostatic I—t transients for nucleation and growth of NiFe film

The most extensively employed theoretical model for electrochemical nucleation is the one developed by Hills and his colleagues[23]. Even though this theoretical model is based on the nucleation/growth of single metal, it has been widely used to analyze the nucleation/growth of alloys[8, 26, 27]. In this model[19-23], the authors describe the kinetics of electrolytic phase formation at early stages when diffusion of the electroactive species from bulk solution to the interface is the rate determining step, and the growth of nuclei is considered to be 3D taking into account of the overlap of diffusion zones. According to this model, the rising portion of the current transient can be described, respectively for the instantaneous nucleation and progressive nucleation by

$$I_i = zFD^{1/2}c[1-\exp(-N\pi kDt)]/\pi^{1/2}t^{1/2} \quad (1)$$

$$k = [8\pi cM/\rho]^{1/2} \quad (2)$$

$$I_p = zFD^{1/2}c[1-\exp[-AN_\infty\pi k'Dt^2/2]]/\pi^{1/2}t^{1/2} \quad (3)$$

$$k' = 4[8\pi cM/\rho]^{1/2}/3 \quad (4)$$

where zF is the molar charge of electrodepositing species, D is the diffusion coefficient, c is the bulk concentration of the zinc species, N is the number of nuclei, N_∞ and AN_∞ are the total number of active sites for instantaneous nucleation and progressive nucleation respectively, M is the molar mass, ρ is the density of the deposited material, and k and k' are the numerical constants determined by the experimental conditions.

Fig. 3 shows the relationship of the experimental non-dimensional variables between (t/t_m)

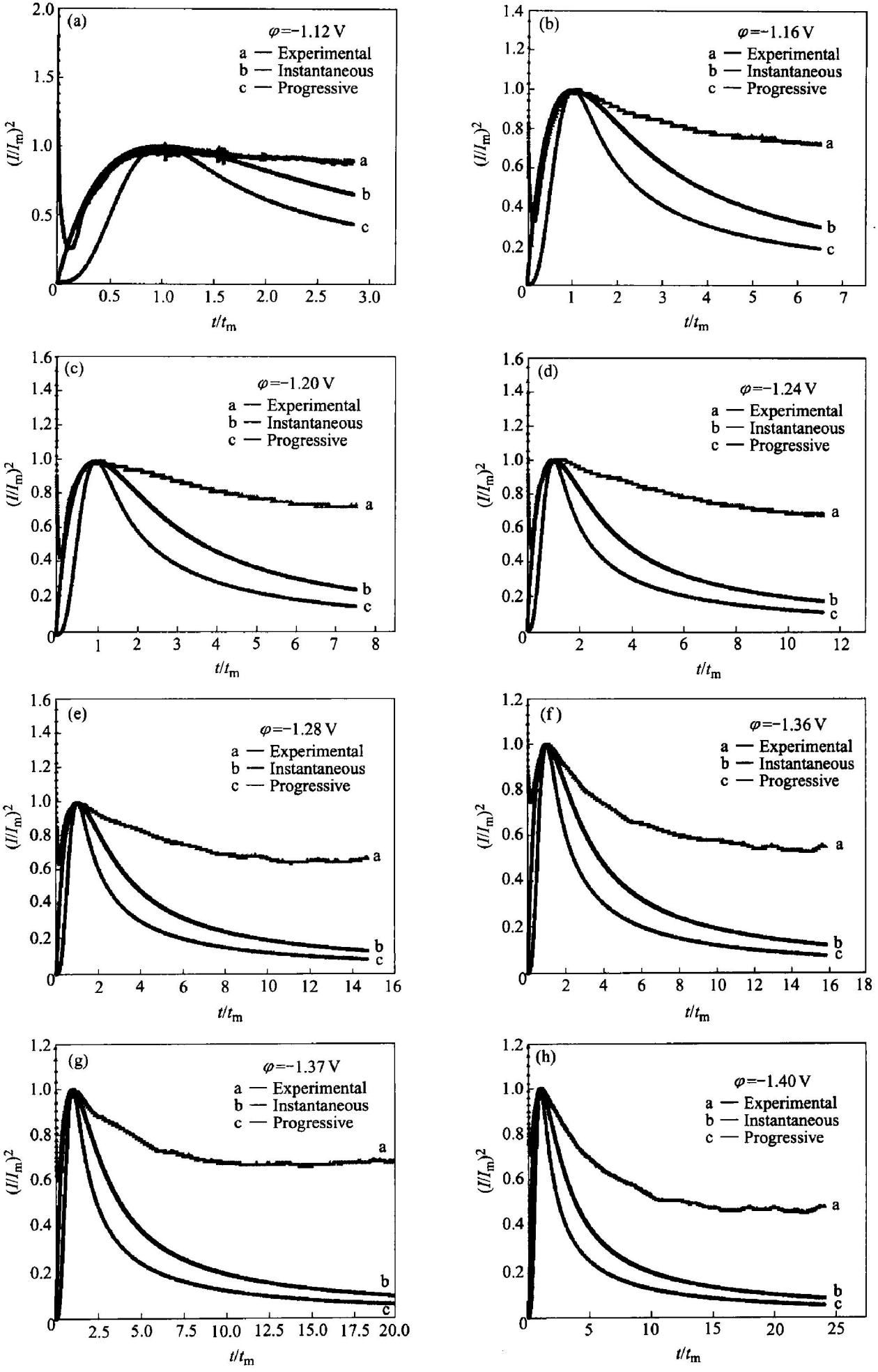

Fig. 3 Non-dimensional I/I_{max} vs t/t_{max} plots for electrodeposition of NiFe film

and $(I/I_m)^2$, where I_m and t_m are the current transient maximum values. Determination of the nucleation/growth process involved is achieved by analyzing the rising section of the current transient and then comparing the curve to the dimensionless theoretical curves obtained from Eqns. (1)–(3) respectively.

From Fig. 3, it can be seen that, in the case of high overpotentials, the experimental $I-t$ curves closely follow the theoretic instantaneous nucleation curves. However, at low overpotential (Fig. 2), no distinguished nucleation current can be observed because the practical electrode substrate surfaces usually possess many imperfections such as plateau edges, kinks, vacancies and emergent screw dislocations, at which crystal growth can occur without nucleation[28].

Meanwhile, it can also be seen from Fig. 3 that, after the maximum current, the experimental $(I/I_m)^2$ is much larger than that calculated from the theoretical model. According to the well accepted theorem, the electrochemical reduction of iron-group metal ions on the cathode surface obeys the following mechanism[29]:

$$2H_2O + 2e^- \rightarrow H_2 + 2OH^- \quad (5)$$

$$M^{2+} + OH^- \rightarrow M(OH)^+ \quad (6)$$

$$M(OH)^+ \rightarrow M(OH)^+_{ads} \quad (7)$$

$$M(OH)^+_{ads} + 2e^- \rightarrow M + OH^- \quad (8)$$

where M designates iron, cobalt and nickel atoms. Therefore, the reduction rate of M mainly depends on the stability of $M(OH)^+_{ads}$ or $M(OH)^+$, i.e. the atomic orbital (Φ_A and Φ_B) overlapping integral ($S_{A\text{-}B}$) of M and O in OH^-. The larger the $S_{A\text{-}B}$, the more stable the $M(OH)^+_{ads}$ or $M(OH)^+$. According to the theory of molecular orbital[30], $S_{A\text{-}B}$ is directly proportional to the product of the radial function of the two bonding atoms ($R_{n,l,r_A} \cdot R_{n,l,r_B}$)

$$S_{A\text{-}B} \propto R_{n,l,r_A} \cdot R_{n,l,r_B} \quad (9)$$

Because the energy of the empty 3d-orbit is less than that of 4s-orbit, the first electron from the cathode will fill into the 3d-orbit preferentially. In this case, the empty orbit of the monovalent iron-base metal ions in $M(OH)^+_{ads}$ will be the 4s-orbit. For the 4s-orbital of Fe and Ni,

$$\frac{dR}{dr} < 0 \quad (10)$$

Therefore, $R_{n,l,r}$ decreases with the increase of the atomic radius (r) of iron series elements. Because the radii of iron series ions (M^{2+}) follow the following order[31]: $r_{Fe} > r_{Ni}$ (Table 2), then $S_{O-Ni} > S_{O-Fe}$, i.e. the stability of the iron-group metal monohydroxide ions or metal hydroxides can be sorted in the following order: $Ni(OH)^+ > Fe(OH)^+$, which will result in the anomalous co-deposition of nickel-iron binary alloys. The above stability order of the nickel and iron metal monohydroxide ions or metal hydroxides are also supported by calculating the crystal field stabilizing energy (CFSE) of $Ni(OH)^+$ and $Fe(OH)^+$ using GAUSSIAN94 software[32], on the basis of the electrodeposition mechanism shown in Eqns. (5)–(8) and that, under our electroplating conditions, the OH^- ions are a kind of weak ligands which will result in high spin ligated compounds[33] (Table 2).

Table 2 Radii of iron-group ions (M^{2+})[32] and CFSE of $Ni(OH)^+$ and $Fe(OH)^+$

Ion	Radius/m	CFSE/2.721 eV
Fe^{2+} / $Fe(OH)^+$	7.5×10^{-11}	−0.753 088
Ni^{2+} / $Ni(OH)^+$	7.0×10^{-11}	−0.656 686

Because the stability of the nickel and iron metal monohydroxide ions or metal hydroxides can be sorted in the following order: $Ni(OH)^+ > Fe(OH)^+$ as elucidated above, the content of nickel in the electrodeposited film is much lower than that in the electroplating solution, and the concentration of Ni^{2+} in the vicinity of the cathode should maintain at a relatively steady value during the whole electroplating process. Therefore, the experimental $(I/I_m)^2$ should be much larger than that calculated from the theoretical model; while the decrease of current after the current maximum in $I-t$ curves may be originated from the sparsity of Fe^{2+} ions on the cathode surface.

4 CONCLUSIONS

Under the experimental conditions, the electroplating of Ni-Fe alloy follows 3-D nucleation/growth mechanism. In the case of high deposition overpotential, the nucleation/growth of Ni-Fe alloy is instantaneous, and the growth rate of the previously formed nuclei increases with overpotential. However, at low overpotential, no distinguished nucleation current can be observed and crystal growth can occur without nucleation. The discrepancy between the experimental non-dimensional variables $(I/I_m)^2$ and those calculated from the theoretical model can be theoretically contributed to the fact that the orbital radius of 4s of nickel atom is shorter than that of iron atom and the stability of the iron-group metal monohydroxide ions or metal hydroxides can be sorted in the following order: $Ni(OH)^+ > Fe(OH)^+$.

REFERENCES

[1] Kieling V C. Parameters influencing the electrodeposition of Ni-Fe alloys [J]. Surf Coat Technol, 1997, 96: 135–139.

[2] Cheung C, Djuanda F, Erb U, et al. Electrodeposition of nanocrystalline Ni-Fe alloys [J]. Nanostructured Materials, 1995, 5(5): 513-523.
[3] Grimmett A, Schwartz M, Nobe K. A comparison of DC and pulsed Fe-Ni alooy deposits [J]. J Electrochem Soc, 1993, 140(4): 973-978.
[4] Horkans J. Effect of plating parameters on electrodeposited NiFe [J]. J Electrochem Soc, 1981, 128(1): 45-49.
[5] Andricocos P C, Arana C, Tabib J, et al. J Electrochem Soc, 1989, 136(5): 1336-1340.
[6] Grimmett D L, Schwartz M, Nobe K. Pulsed electrodeposition of iron-nickel alloys [J]. J Electrochem Soc, 1990, 137(11): 3414-3418.
[7] Matlosz M. Competitive adsorption effects in the electrodeposition of iron-nickel alloys [J]. J Electrochem Soc, 1993, 140(8): 2272-2279.
[8] Afshar A, Dolati A G, Ghorbani M. Electrochemical characterization of the Ni-Fe alloy electrodeposition from chloride-citrate-glycolic acid solution [J]. Mater Chem Phys, 2002, 77: 352-358.
[9] Schultz H, Pritzker M. Modeling the galvanostatic pulse and pulse reverse plating of nickel-iron alloys on a rotating disk electrode [J]. J Electrochem Soc, 1998, 145(6): 2033-2042.
[10] Hessami S, Tobias C W. A mathematical model for anomalous codeposition of nickel-iron on a rotating disk electrode [J]. J Electrochem Soc, 1989, 136(12): 3611-3616.
[11] Yang Z N, Zhang Z, Zhang J Q, et al. Electrodeposition behavior of nanocrystallization CoNiFe soft magnetic thin film [J]. Surf Coat Technol, 2005, 198(1): 11-16.
[12] Margarita M H, Manuel P P, Nikola B, et al. Identification of different silver nucleation processes on vitreous carbon surfaces from an ammonia electrolytic bath [J]. J Electroanal Chem, 1998, 443: 81-93.
[13] Manuel P P, Margarita M H, Ignacio G, et al. Detailed characterization of potentiostatic current transients with 2D-2D and 2D-3D nucleation transitions [J]. Surf Sci, 1998, 399: 80-95.
[14] Enrique B, Manuel P P, Nikola B, et al. Formation mechanisms and characterization of black and white cobalt elctrodeposition onto stainless steel [J]. J Electrochem Soc, 2000, 147(5): 1787-1796.
[15] Manuel P P, Ma T R, Ignacio G. Silver electrocrystallization on vitreous carbon from ammonium hydroxide solutions [J]. J Electrochem Soc, 1996, 143(5): 1551-1546.
[16] Gunawardena G, Hills G, Montenegro I, et al. Electrochemical nucleation — Part Ⅰ. General considerations [J]. J Electroanal Chem, 1982, 138: 225-239.
[17] Holzle M H, Retter U, Kolb D M. The kinetics of structural changes in Cu adlayers on Au(111) [J]. J Electroanal Chem, 1994, 371: 101-109.
[18] Manuel P P, Ignacio G, Nikola B. New insights into evaluation of kinetic parameters for potentiostatic metal deposition with underpotential and overpotential deposition processes [J]. J Phys Chem B, 2000, 104: 3545-3555.
[19] Gunawardena G, Hills G, Montenegro I, et al. Electrochemical nucleation — Part Ⅲ. The electrodeposition of mercury on vitreous carbon [J]. J Electroanal Chem, 1982, 138: 255-271.
[20] Hills G J, Schiffrin D J, Thompson J. Electrochemical nucleation from molten salts — Ⅰ. Diffusion controlled electrodeposition of silver from alkali molten nitrates [J]. Electrochim Acta, 1974, 19: 657-670.
[21] Scharifker B, Hills G. Theoretical and experimental studies of multiple nucleation [J]. Electrochim Acta, 1981, 28: 879-889.
[22] Scharifker B, Mostany J. Three-dimensional nucleation with diffusion controlled growth — Part Ⅰ. Number density of active sites and nucleation rates per site [J]. J Electroanal Chem, 1984, 177: 13-23.
[23] Fletcher S, Halliday C S, Gates D, et al. The response of some nucleation/growth processes to triangular scans of potential [J]. J Electroanal Chem, 1983, 159: 267-285.
[24] ZHANG Zhao. Electrochemical behavior of electroplated Zn-P alloy [J]. Trans Nonferrous Met Soc China, 2001, 11(4): 603-605.
[25] Zhang Z, Leng W H, Shao H B, et al. Study on the behavior of Zn-Fe alloy electroplating [J]. J Electroanal Chem, 2001, 516: 127-130.
[26] Petersson I, Ahlberg E. Kinetics of the electrodeposition of Pb-Sn alloys(Part Ⅰ) —At glassy carbon electrodes [J]. J Electroanal Chem, 2000, 485: 166-177.
[27] Petersson I, Ahlberg E. Kinetics of the electrodeposition of Pb-Sn alloys(Part Ⅱ) —At polycrystalline gold electrodes [J]. J Electroanal Chem, 2000, 485: 178-187.
[28] Schindler W, Hugelmann P, Hugelmann M, et al. Localized electrochemical nucleation and growth of low-dimensional metal structures [J]. J Electroanal Chem, 2002, 522: 49-57.
[29] Tsay P, Hu C C. Non-anomalous codeposition of iron-nickel alloys using pulse-reverse electroplating through means of experimental strategies [J]. J Electrochem Soc, 2002, 149(10): C492-C497.
[30] Zhang Z, Leng W H, Li J F, et al. Cooperation behavior of iron and phosphorus in electrodeposition of zinc-iron-phosphorus coatings [J]. Mater Chem Phys, 2002, 77: 497-500.
[31] Liu C K. Inorganic Chemistry(Vol. Ⅰ) [M]. Changsha: Central South University of Technology Press, 1994. 182.
[32] Frisch M J, Trucks G W, Schlegel H B, et al. Gaussian 94, Revision E. 1 [M]. Pittsburgh PA: Gaussian Inc, 1995.
[33] Jiang Y S. The Structure Chemistry [M]. Beijing: High Education Press, 1997. 197-202.

(Edited by YANG Bing)